Expanded View Figures

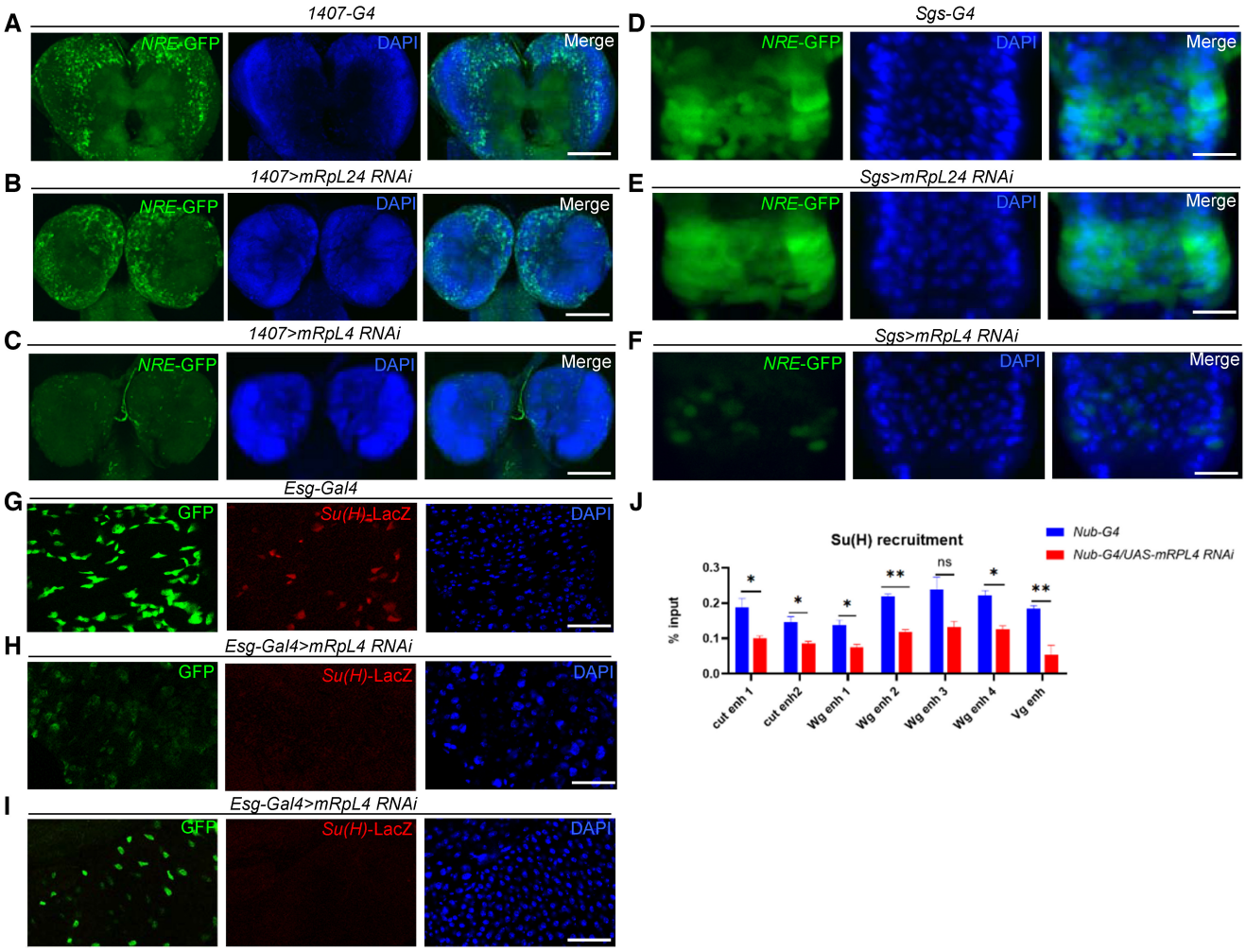

Figure EV1. Effects of mRpL4 RNAi on Notch signal activity.

A–C Representative image showing the expression of *NRE*-GFP in larval neuroblasts ($n > 10$ larvae) of control (A), mRpL24 RNAi (B) and mRpL4 RNAi (C) larvae.

D–F Representative image showing the expression of *NRE*-GFP in salivary gland imaginal rings ($n > 10$ larvae) of control (D), mRpL24 RNAi (E) and mRpL4 RNAi (F) larvae.

G–I Representative image showing the expression of *Su(H)*-LacZ in midgut cells ($n > 10$ flies) of control (G) and mRpL4 RNAi (H, I) adult flies.

J The level of Su(H) occupancy at *Wg*, *Cut* and *Vg* genomic regions as assessed by qPCR following ChIP, from wild-type and *UAS-mRpL4-RNAi*-expressing wing disks. Data are presented as mean ± SEM, two biological replicates for each genotype and three technical replicates for each sample. Statistical significance was tested using two-tailed unpaired *t*-test. *$P < 0.05$, **$P < 0.01$, ns means "not significant".

Data information: Scale bars = 100 μm.

Figure EV2. Effects of overexpressing Notch signaling components.

A–D Representative image of wing imaginal disks ($n > 10$ wing disks) containing MARCM clones stained for Wg. Notch signaling ligand Dl is overexpressed in wild-type (A) or $mRpL4^{K14608}$ mutant (B) cells. Notch signaling ligand Ser is overexpressed in wild-type (C) or $mRpL4^{K14608}$ mutant (D) cells.

E–H Representative image of wing imaginal disks ($n > 10$ wing disks) containing MARCM clones stained for NICD. Full-length Notch protein (N^{FL}) (E), NEXT (F) and NICD (G) are overexpressed in $mRpL4^{K14608}$ mutant cells. Blank MARCM clones are generated in the wild-type wing disks (H).

Data information: The MARCM clones are marked by GFP and representative clones are marked by white arrows. Scale bars = 100 μm.

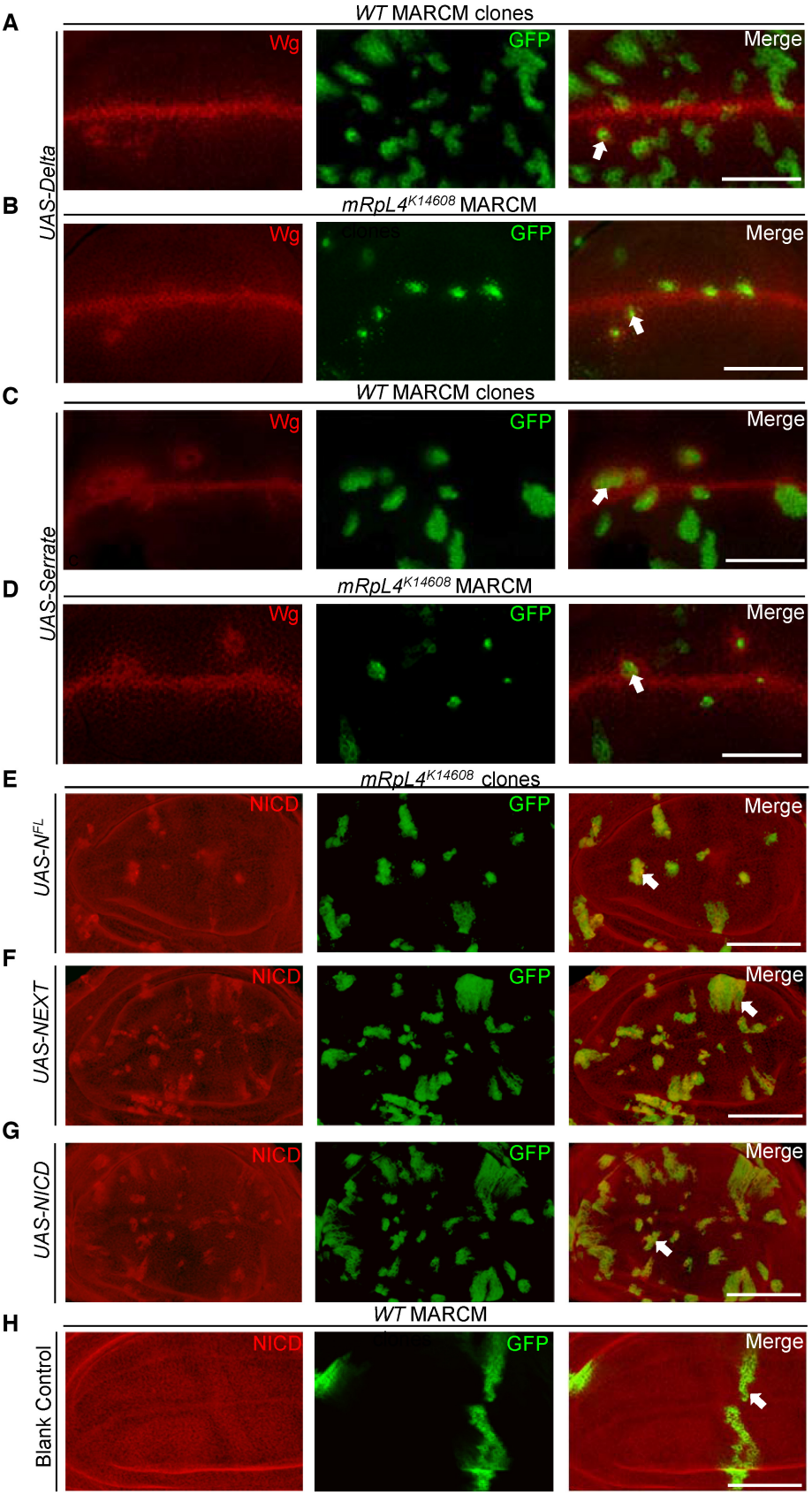

Figure EV2.

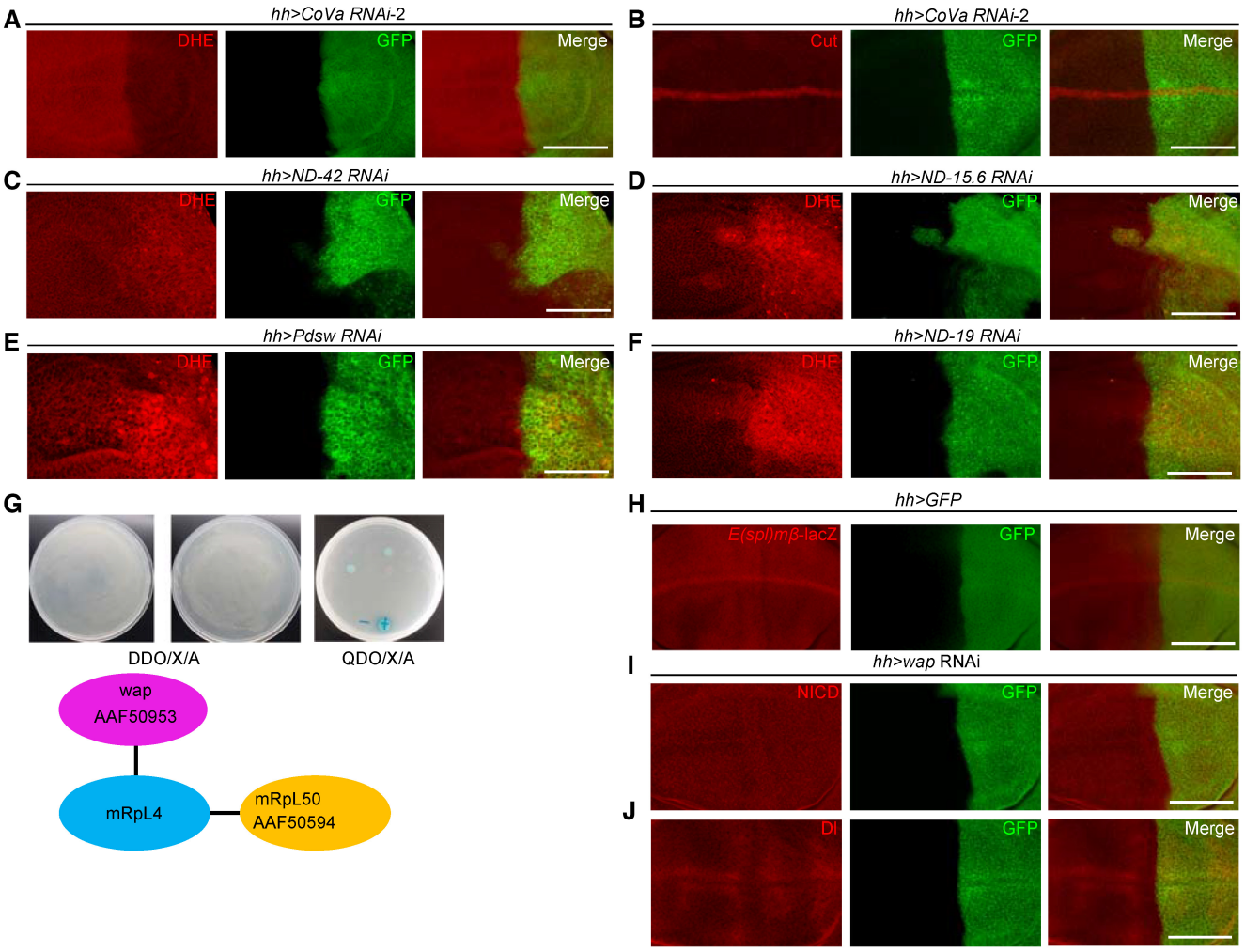

Figure EV3. mRpL4 may regulate OXPHOS activity and Notch signaling through branched pathways.

A, B Representative images of wing imaginal disks (n > 15 wing disks) expressing *CoVa* RNAi under the control of *hh-gal4* (marked by GFP) that are stained for DHE (*A*) and Cut (*B*).

C–F Representative images of wing imaginal disks (n > 20 wing disks) stained by DHE. The expression of *ND-42* (C), *ND-15.6* (D), *Pdsw* (E) and *ND-19* (F) RNAi are under the control of *hh*-Gal4 (marked by GFP).

G Two proteins, mRpL50 and wap are isolated as mRpL4 interaction partners through yeast two-hybridization. The GenBank accession numbers assigned to mRpL50 and wap are AfAF50594 and AAF50953.

H Representative image of wing imaginal disks (n > 15 wing disks) showing *E(spl)mβ*-LacZ expression pattern, and cells in the posterior compartment are marked by GFP.

I, J Representative image of wing imaginal disks (n > 15 wing disks) stained for NICD (I) and Dl (J). In these wing disks, *wap* RNAi are expressed under the control of *hh*-Gal4 (marked by GFP).

Data information: Scale bars = 100 μm.

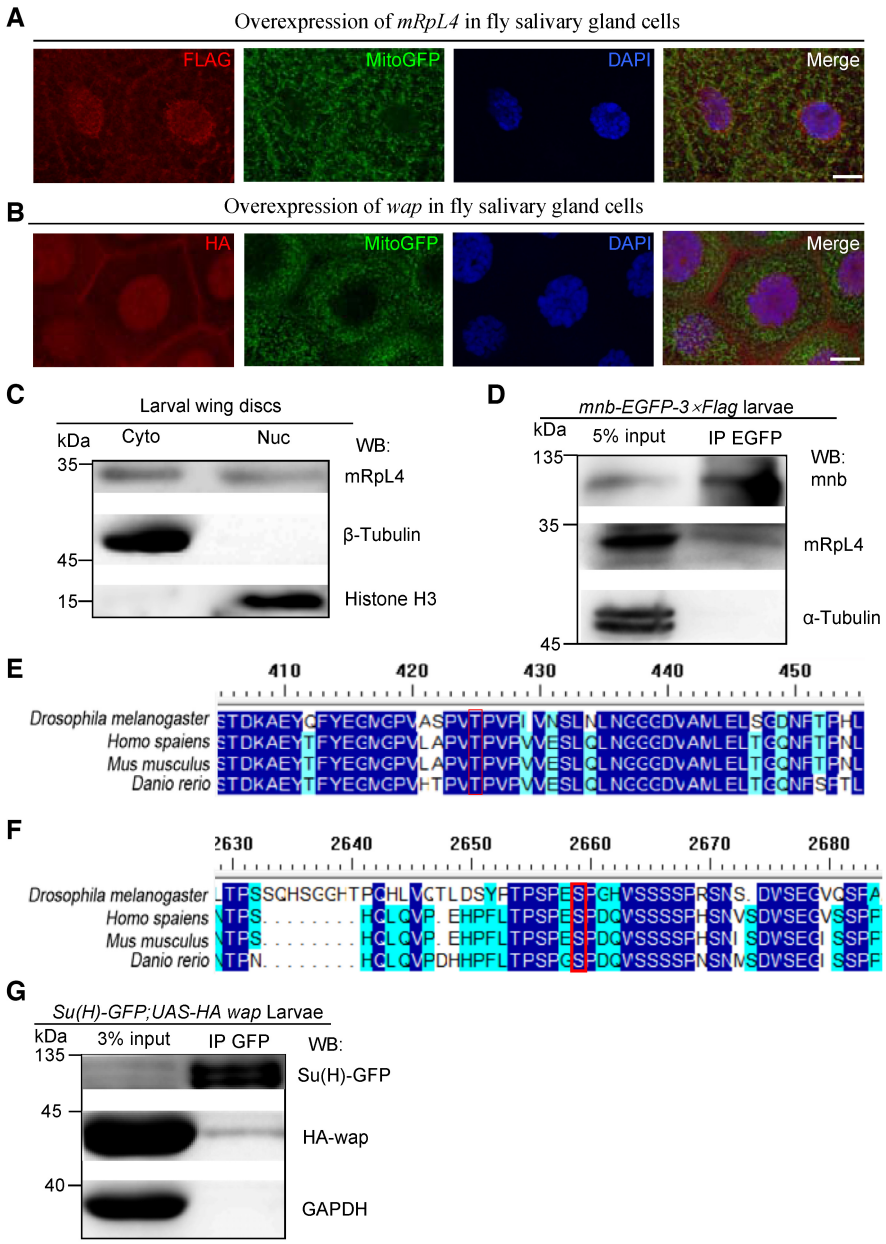

Figure EV4. mRpL4 and wap may function through Su(H) to regulate Notch signaling.

A, B Representative images of third instar larvae salivary glands (n > 10 larvae) from flies expressing FLAG-tagged mRpL4 (A) and HA-tagged wap (B). Immunostaining was performed using anti-FLAG and anti-HA antibodies to reveal mRpL4 and wap, respectively. Mitochondria are marked by GFP and cell nuclei are labeled by DAPI.

C Representative western blotting (n = 3 biological replicates) of mRpL4 protein distribution in cytoplasmic (Cyto) and nuclear (Nuc) fractions from wing disks lysates.

D Representative immunoprecipitation analysis (n = 3 biological replicates) using lysates from wing disks expressing GFP-tagged mnb. Anti-GFP antibodies were used for immunoprecipitation. Western blotting was performed using anti-GFP and anti-mRpL4 antibodies to reveal mnb and mRpL4, respectively. α-Tubulin was used as control.

E Alignment of Su(H) protein sequences from fly, human, mice and zebrafish. The region covering the mnb phosphorylation consensus sequence is shown, and the conserved Thr residue (T426) is labeled by red box.

F Alignment of Notch protein sequences from fly, human, mice and zebrafish. The region covering the mnb phosphorylation consensus sequence is shown, and the conserved Ser residue (S2659) is labeled by red box.

G Representative immunoprecipitation analysis (n = 2 biological replicates) using lysates from wing disks expressing GFP-tagged Su(H) and HA-tagged wap. Anti-GFP antibodies were used for immunoprecipitation. Western blotting was performed using anti-GFP and anti-HA antibodies to reveal Su(H) and wap, respectively. GAPDH was used as control.

Data information: Scale bars = 50 μm in (A and B).
Source data are available online for this figure.

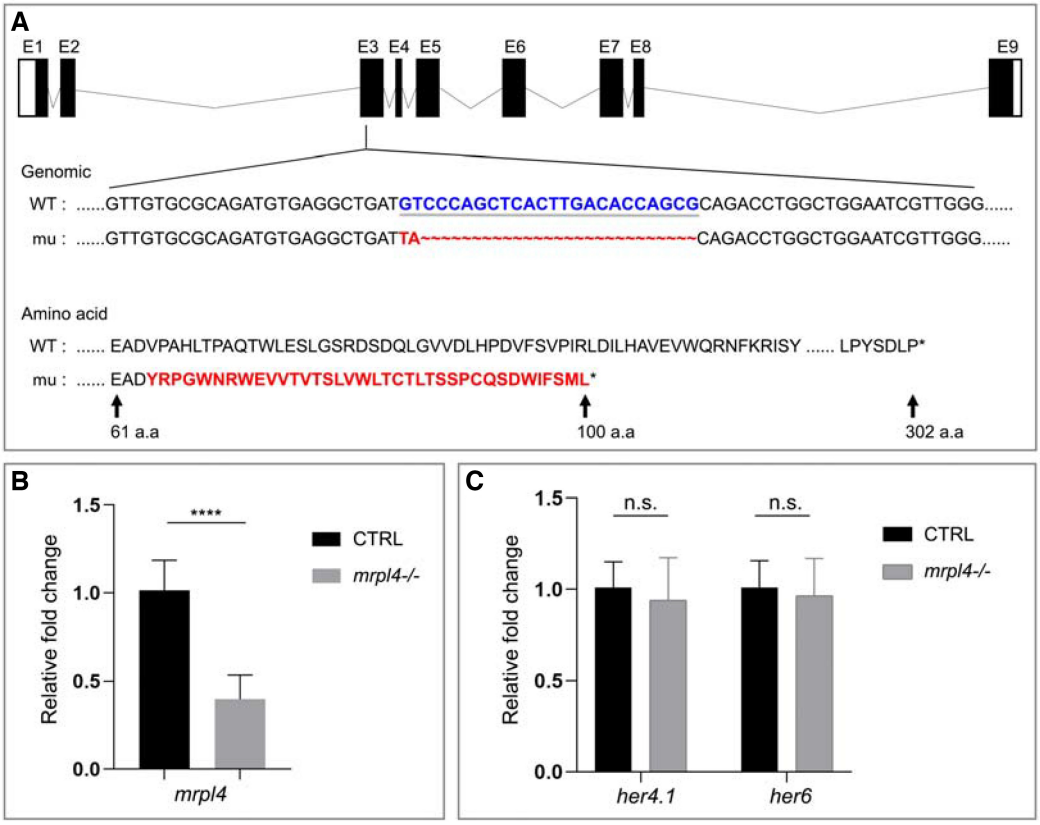

Figure EV5. Function of mRpL4 in zebrafish.

A Schematic diagrams of wild-type (WT) and the *zmRpL4* mutant allele (mu) generated by the CRISPR-Cas9 genome editing system. The mutant allele contains a 24-bp deletion (GTCCCAGCTCACTTGACACCAGCG, in blue) and a 2-bp insertion (TA, in red) in the third exon. As a result, the mutant allele encodes a small polypeptide of 100 amino acid residues containing part of the wild-type residues and a disordered Carbon-terminal tail due to frame shifting (amino acid, in red).

B The mRNA levels of *zmRpL4* in wild-type control and *mrpl4*-null larvae at 5 dpf as measured by quantitative PCR (three biological replicates for each genotype and three technical replicates for each sample). Statistical significance was tested using two-tailed unpaired *t*-test. Error bars represent ± SD, ****$P < 0.00001$.

C Bar graph showing relative levels of Notch signaling target genes *her4.1* and *her6* in *mrpl4*-null larvae comparing to wild-type control at 5 dpf as measured by quantitative PCR ($n = 3$ biological replicates per group). Statistical significance was tested using two-tailed unpaired *t*-test. Error bars represent ± SD; n.s., not significant.

